Hydrol. Earth Syst. Sci. Discuss., 10, 2141–2181, 2013
www.hydrol-earth-syst-sci-discuss.net/10/2141/2013/
doi:10.5194/hessd-10-2141-2013

Hydrology and Earth System Sciences Discussions
Open Access

Development and comparative evaluation of a stochastic analog method to downscale daily GCM precipitation

S. Hwang[1,2] **and W. D. Graham**[1,2]

[1]Department of Agricultural and Biological engineering, University of Florida, Gainesville, Florida, USA
[2]Water institute, University of Florida, Gainesville, Florida, USA

Received: 25 January 2013 – Accepted: 11 February 2013 – Published: 20 February 2013

Correspondence to: S. Hwang (aceace111@ufl.edu)

Published by Copernicus Publications on behalf of the European Geosciences Union.

Abstract

There are a number of statistical techniques that downscale coarse climate information from global circulation models (GCM). However, many of them do not reproduce the small-scale spatial variability of precipitation exhibited by the observed meteorological data which can be an important factor for predicting hydrologic response to climatic forcing. In this study a new downscaling technique (bias-correction and stochastic analog method, BCSA) was developed to produce stochastic realizations of bias-corrected daily GCM precipitation fields that preserve the spatial autocorrelation structure of observed daily precipitation sequences. This approach was designed to reproduce observed spatial and temporal variability as well as mean climatology.

We used the BCSA method to downscale 4 GCM precipitation predictions from 1961 to 1999 over the state of Florida and compared the skill of the method to the results obtained with the commonly used bias-correction and spatial disaggregation (BCSD) approach, bias-correction and constructed analog (BCCA) method, and a modified version of BCSD which reverses the order of spatial disaggregation and bias-correction (SDBC). Spatial and temporal statistics, transition probabilities, wet/dry spell lengths, spatial correlation indices, and variograms for wet (June through September) and dry (October through May) seasons were calculated for each method.

Results showed that (1) BCCA underestimated mean climatology of daily precipitation while the BCSD, SDBC and BCSA methods accurately reproduced it, (2) the BCSD and BCCA methods underestimated temporal variability because of the interpolation and regression schemes used for downscaling and thus, did not reproduce daily precipitation standard deviations, transition probabilities or wet/dry spell lengths as well as the SDBC and BCSA methods, and (3) the BCSD, BCCA and SDBC methods underestimated spatial variability in precipitation resulting in under-prediction of spatial variance and over-prediction of spatial correlation, whereas the new stochastic technique (BCSA) accurately reproduces observed spatial statistics for both the wet and dry seasons. This study underscores the need to carefully select a downscaling method that

HESSD
10, 2141–2181, 2013

reproduces all precipitation characteristics important for the hydrologic system under consideration if local hydrologic impacts of climate variability and change are going to be accurately predicted. For low-relief, rainfall-dominated watersheds where reproducing small-scale spatiotemporal precipitation variability is important, the BCSA method is recommended for use over the BCSD, BCCA, or SDBC methods.

1 Introduction

General circulation models (GCMs) are considered robust tools for simulating future changes in climate and for developing climate scenarios for quantitative impact assessments (Wilks, 1999; Karl and Trenberth, 2003; Fowler et al., 2007). General circulation modeling continues to be improved by the incorporation of more aspects of the complexities of the global system. However, GCM results are generally insufficient to provide accurate prediction of climate variables on the local to regional scale needed to assess hydrologic impacts because of significant uncertainties in the modeling process (Allen and Ingram, 2002; Didike and Coulibaly, 2005). The coarse resolution of existing GCMs (typically about 200 km by 200 km) precludes the simulation of realistic circulation patterns and accurate representation of the small-scale spatial variability of climate variables (Christensen and Christensen, 2003; Giorgi et al., 2001; Johns et al., 2004; Lettenmaier, 1999; Wood et al., 2002). Furthermore, mismatch of the spatial resolution between GCMs and hydrologic models generally precludes the direct use of GCM outputs to predict hydrologic impacts.

To overcome this limitation of GCMs, a number of downscaling methods have been developed. It has been shown that fine-scale downscaled results provide better skill for hydrologic modeling (Andréasson et al., 2004; Graham et al., 2007; Wood et al., 2004) and agricultural crop modeling (Mearns et al., 1999, 2001) than using the coarse-resolution GCM output directly. Often downscaling techniques use statistical methods that employ empirical relations between features simulated by GCMs at large grid scales and surface observations at sub-grid scales (Hay et al., 2002; Wilby and Wigley,

HESSD
10, 2141–2181, 2013

1997). The primary advantage of these techniques is that they are computationally inexpensive, and thus can be easily applied to multiple GCM simulations. Additionally statistical downscaling has been shown to provide climate information at any specific resolution of interests so that is the outcome may be directly used for many climate change impact studies (Fowler et al., 2007; Murphy, 1999; Wilby et al., 2004).

Although much progress on downscaling precipitation sequences has been made, current challenges include the need to represent realistic levels of temporal and spatial variability at multiple scales (e.g. daily, seasonal and inter-annual variability, Timbal et al., 2009) in the generated sequences, the simultaneous downscaling of correlated climate variables (i.e. precipitation and temperature, Zhang and Georgakakos, 2012), and the accurate representation of extreme events (Yang et al., 2012; Katz and Zheng, 1999). In particular, accurately representing the spatial variability and patterns of precipitation can be an important factor for predicting hydrologic response to climatic forcing at the watershed scale, especially in low-relief watersheds affected by convective storm systems as in Florida (Hwang et al., 2011; Smith et al., 2004).

Statistical downscaling approaches are often applied at a temporally aggregated scale (e.g. monthly or seasonally) rather than daily or sub-daily time scales because of distortion of GCM daily results (Maurer and Hidalgo, 2008). When applied at a daily time scale, the direct use of GCM results makes them quite susceptible to model biases (Ines and Hansen, 2006). Means of addressing the problem include aggregating GCM predictions into seasonal or sub-seasonal means, downscaling to the target grid scale or station network, and then using a weather generator (Wilks, 2002; Wood et al., 2004; Feddersen and Andersen, 2005) or analog methods which re-sample the historic data to disaggregate in time (Salathe et al., 2007; Maurer et al., 2010; Zhang and Georgakakos, 2012). Generally using a weather generator to generate daily climate sequences exhibits no skill at reproducing spatial correlation and is also limited by the assumption that current temporal daily patterns of precipitation will be preserved in the future (Fowler et al., 2007). The use of analogs is constrained by the requirement that a sufficiently long observation record exists so that reasonable analogs can be found (Zorita and Storch, 1999).

Bias-corrected spatial downscaling (BCSD Wood et al., 2002; Maurer, 2007) is a widely used technique to downscale GCM results and it has been extensively applied to assess hydrologic impacts of climate change in the US (Christensen et al., 2004; Wood et al., 2004; Salathe et al., 2007; Maurer and Hidalgo, 2008). BCSD generally preserves relationships between large-scale GCM results and local-scale observed mean precipitation trends. Although this method was originally developed for downscaling monthly precipitation and temperature, in principle, daily GCM output can also be downscaled directly using this method. However realistic spatial variability of daily precipitation events may not be reproduced by this method because it is designed to preserve only the observed temporal statistics at the time scale chosen for downscaling and the spatial disaggregation process is essentially a simple interpolation scheme.

The constructed analog method (CA; Hidalgo et al., 2008) is a technique developed to directly downscale daily GCM products to assess hydrologic implications of climate scenarios. Hidalgo et al. (2008) showed that CA exhibited considerable skill in reproducing observed daily precipitation and temperature statistics but underestimated the mean and standard deviation of daily precipitation over the southeast US. Maurer and Hidalgo (2008) compared CA and BCSD method and demonstrated that CA showed better skill than BCSD, particularly in reproducing extreme temperature events. However both methods showed limited skill in reproducing daily precipitation extremes. Subsequently, Maurer et al. (2010) introduced the bias-correction and constructed analog (BCCA) method which improved the CA method by removing the biases attributed to GCMs and showed better accuracy in simulating hydrologic extremes.

Abatzoglou and Brown (2012) modified the BCSD method by changing the order of the bias-correction and spatial disaggregation procedures. That is, they interpolated GCM outputs onto a fine grid first and then the fields were bias-corrected using the CDF mapping approach for each fine scale grid cell (i.e. the target resolution of downscaling). This simple modification (hereafter referred to as SDBC) improved the

HESSD
10, 2141–2181, 2013

downscaling skill for reproducing local-scale temporal statistics. However the SDBC method does little to improve skill in reproducing spatial variability because the same approach (interpolation) as used in BCSD is employed for spatial disaggregation.

The ultimate goal of this study was to improve the existing bias-correction based downscaling methods introduced above by introducing a method that preserves both spatial and temporal statistics of daily precipitation with similar computational cost. This paper presents a new stochastic generation technique (bias-correction and stochastic analog method, hereafter BCSA) to produce downscaled daily GCM precipitation predictions. BCSA is then used to downscale precipitation predictions from 4 retrospective GCM simulations over Florida and the skill of the method is comparatively evaluated to the downscaled results obtained using the BCSD, BCCA, and SDBC techniques.

2 Data

Daily gridded observations at 1/8 degree spatial resolution (about 12 km) were obtained over Florida from 1950 to 1999 (Maurer et al., 2002). The climate data (daily and monthly precipitation, maximum, minimum, and average temperature, and wind speed) are archived in netCDF format at http://hydro.engr.scu.edu/files/gridded_obs/daily/ncfiles/. These products are available from 1950 through 1999 over the entire US. without missing data. This data was used to bias-correct daily GCM results and to estimate observed spatial correlation structure.

GCM data from 1961 to 1999 were obtained from the World Climate Research Programme's (WCRP's) Coupled Model Inter-comparison Project phase 3 (CMIP3) multi-model dataset, which are referenced in the Intergovernmental Panel on Climate Change (IPCC) Fourth Assessment Report (AR4, 2007). The GCMs selected for this study are shown in Table 1. The grid resolutions for the GCMs range from 1.4° to 2.8°. Figure 1 shows how each model grid configuration covers the study domain over Florida.

HESSD
10, 2141–2181, 2013

3 Statistical downscaling methods

3.1 Bias-correction and spatial downscaling at daily scale (BCSD_daily) method

The BCSD method is an empirical statistical technique that was developed by Wood et al. (2002). As described above, the method was originally designed to downscale monthly precipitation and temperature, but daily GCM output can also be directly applied using this method. In this study, we employed same methodology but at daily time scale and evaluated the skills in reproducing the spatiotemporal mean and variability of daily precipitation. The technique will be referred to as the BCSD_daily hereafter. BCSD_daily consists of two separate steps for bias-correction and spatial downscaling. In the first step, raw GCM predictions are bias-corrected at the large GCM grid scale using the CDF mapping approach (Panofsky and Brier, 1968, described in detail in the next paragraph). In the second step anomalies (i.e. the ratio of simulated precipitation field to observed temporal mean precipitation field) of the bias-corrected GCM output are spatially interpolated to the downscaled resolution using an inverse distance weighting technique (Shepard, 1984). Finally these fine-scale anomalies are re-scaled with the mean precipitation field at the fine grid scale resolution.

The bias-correction procedure used in the BCSD_daily method is similar to that used by Wood et al. (2002); Ines and Hansen (2006); Salathe et al. (2007); and Maurer and Hidalgo (2008) and is described as follows: (1) CDFs of observed daily precipitation at the coarse GCM scale were created individually for each month using the spatial average of available observed data from Maurer et al. (2002) within each GCM grid. Thus 12 observed monthly CDFs were created for each GCM grid cell; (2) CDFs of simulated daily precipitation were created for each grid cell for each month; (3) daily grid cell predictions were bias-corrected at the large-scale GCM prediction resolution using CDF mapping that preserves the probability of exceedence of the simulated precipitation over the grid cell, but corrects the precipitation to the value that corresponds to the same probability of exceedence from the spatially averaged observation over the GCM grid. Thus bias-corrected rainfall $x'_{t,i}$ on day t at grid i was calculated as,

HESSD
10, 2141–2181, 2013

A stochastic analog downscaling method

S. Hwang and W. D. Graham

$$x'_{t,i} = F^{-1}_{\mathrm{obs},i}(F_{\mathrm{sim},i}(x_{t,i})) \tag{1}$$

where $F(x)$ denote the CDF of daily precipitation x, and its inverse, and subscripts sim and obs indicate GCM simulation and observed daily rainfall, respectively. This bias-correction process removes both bias in the precipitation predictions and the tendency of the model to under-predict dry days and over-predict the number of low volume rainfall days (Hwang et al., 2011).

3.2 Bias-correction and constructed analog (BCCA) method

The constructed analog (CA) technique creates a library of observed daily coarse-resolution climate anomaly patterns for the variable to be downscaled, then selects a set of analogs with patterns that closely match the simulated anomaly pattern that must be downscaled. A linear combination of the selected observed daily coarse-resolution climate anomalies patterns is used to estimate a coarse resolution analog to the simulated anomaly, and a downscaled anomaly is generated by applying the same linear combination to the corresponding set of high resolution observed climate anomaly patterns. The CA approach retains daily sequencing of weather events from the GCM results and various possible climate variables (e.g. geopotential heights, sea level pressure) can be considered as predictors to construct the best analog. A significant limitation of the CA approach, as originally developed, is that the biases exhibited by the GCM (resulting from imperfect model parameterization of physical processes or inadequate topographic description in the model) are reconstructed in the downscaled fields (Hidalgo et al., 2008; Maurer and Hidalgo, 2008). In order to overcome this drawback, Maurer et al. (2010) suggested a hybrid method, BCCA combining statistical bias-correction (as used in BCSD) prior to applying the constructed analog. However, BCCA may not accurately reproduce the mean and variance of precipitation at the downscaled resolution. This is because "anomaly patterns" of the bias-corrected GCM (instead of the bias-corrected GCM, itself) are used to choose analogs and historical records corresponding to the analogs are combined using linear regression without further bias-correction at the fine resolution. In this study, we used previously developed BCCA results available over the entire USA from http://gdo-dcp.ucllnl.org/downscaled_cmip3_projections/. Four GCMs (i.e. GFDL, CGCM, CNRM-CM3, and MIROC3.2) were used from this data set (Table 1). Note that the BCCA results are not available for BCCR-BCM2.0 and CCSM that we used for other statistical methods.

3.3 Spatial downscaling and bias-correction (SDBC) method

The SDBC method developed by Abatzoglou and Brown (2012) was the third previously published methodology evaluated in this study. As described above the SDBC method is a modified version of the BCSD method in which the order of bias-correction and spatial disaggregation is reversed. That is, GCM outputs are interpolated to the fine grid scale using inverse distance weighting first and then the interpolated precipitation fields are bias-corrected using the CDF mapping approach described above but at the local grid scale. This modification improves the downscaling skill in reproducing local temporal statistics since bias-correction is conducted at the local grid scale.

3.4 Bias-correction and stochastic analog (BCSA) method

A new spatial downscaling technique was developed to generate spatially correlated downscaled precipitation predictions which preserve both the temporal statistical characteristics as well as the small-scale spatial correlation structure of observed precipitation fields. The technique will be referred to as the BCSA method hereafter. Because the spatiotemporal features (e.g. frequency, spatial patterns, and correlation) of precipitation events may change monthly or seasonally, the BCSA process was performed using temporal and spatial statistics calculated separately for each month. The procedure for the BCSA method performed for each month is described as follows:

i. Gridded precipitation observations were transformed into standard normal variables using the normal score transformation approach (Goovaerts, 1997; Deutsch and Journel, 1998), i.e.:

$$x^*_{t,i} = G^{-1}(F_{\mathrm{obs},i}(x_{t,i})) \tag{2}$$

where $x^*_{t,i}$ is the normal score for $x_{t,i}$ (i.e. observed daily precipitation on day t at grid i), $G^{-1}(\cdot)$ is the inverse transform function of the standard Gaussian CDF and $F_{\mathrm{obs},i}(x)$ denotes the CDF of daily gridded observation for grid i.

ii. Pearson's correlation coefficients ρ for the normal score transform variables for all pairs of grid cell observations over the study domain were calculated for each month using the following equation:

$$\rho_{i,j} = \frac{1}{N}\frac{\sum_{t=1}^{N}\left(x^*_{t,i} - \overline{x^*_i}\right)\left(x^*_{t,j} - \overline{x^*_j}\right)}{\sigma^*_i \sigma^*_j} \tag{3}$$

where N is the number of data points (days) available for each grid cell, $\overline{x^*_i}$ and σ^*_i denote the temporal mean and standard deviation of normal scores for grid i, respectively. The full correlation matrix that consists of all the calculated pair-wise correlations was then assembled:

$$\rho = \begin{bmatrix} \rho_{1,1} & \cdots & \rho_{1,n} \\ \vdots & \ddots & \vdots \\ \rho_{n,1} & \cdots & \rho_{n,n} \end{bmatrix} \tag{4}$$

where n is the number of grid cells.

iii. The symmetric positive-definite correlation matrix ρ was factored using the Cholesky decomposition method (Taussky and Todd, 2006) that decomposes the

HESSD
10, 2141–2181, 2013

matrix into the product of a lower triangular matrix and its conjugate transpose, i.e.:

$$\rho = \mathbf{L}\mathbf{L}^* \tag{5}$$

where $\mathbf{L}$ is a lower triangular matrix with strictly positive diagonal entries, and $\mathbf{L}^*$denotes the conjugate transpose of $\mathbf{L}$.

iv. Vectors with elements corresponding to each grid cell were randomly generated from independent Gaussian distributions for each day t ($\boldsymbol{r}_t$) then transformed into pair-wise correlated vectors ($\boldsymbol{r}_t^{\varphi}$) by multiplying with the calculated factorization matrix $\mathbf{L}^*$. Note that random vector for each day, $\boldsymbol{r}_t$ contains n elements corresponding to each grid cell.

$$\boldsymbol{r}_t^{\varphi} = \boldsymbol{r}_t \mathbf{L}^* \tag{6}$$

The $\boldsymbol{r_t}^{\varphi}$ generated by this process honor the observed spatial correlation but have zero mean and unit variance.

v. Spatially correlated normal score variables $\boldsymbol{r}_t^{\varphi}$ were back-transformed to their observed distributions using the CDF of the corresponding gridded observation in the following equation:

$$\hat{x}_{t,i} = F_{\text{obs},i}^{-1}(F_{\text{norm},i}(x_{t,i}^{\varphi})) \tag{7}$$

where $x_{t,i}^{\varphi}$ is an element of $\boldsymbol{r}_t^{\varphi}$ for grid i. $F_{\text{norm},i}(\cdot)$ denotes the CDF of generated normal scores for grid i and $\hat{x}_{t,i}$ is the precipitation estimation for day t and grid i. This procedure was repeated for every grid cell to get ensembles of daily precipitation fields that preserve the mean, variance, and spatial correlation structure of the observed field.

vi. Steps 4 and 5 are repeated to create an ensemble of 3000 replicates of spatially distributed precipitation fields for each month.

HESSD
10, 2141–2181, 2013

A stochastic analog downscaling method

S. Hwang and W. D. Graham

vii. For each bias-corrected daily GCM prediction x'_t (obtained using the same bias-correction procedure described above for the BCSD method), a realization was selected from the appropriate monthly ensemble with spatial mean of the generated precipitation fields equal to the GCM prediction.

4 Assessment of downscaling skill

The temporal mean, 50th percentile, 90th percentile, and standard deviation of the precipitation time series for observed and downscaled predictions were calculated for each grid cell and mapped over the state of Florida to evaluate the spatial distribution of these temporal statistics for both the wet season (June through September) and the dry season (October through May). Daily transitions between wet and dry states were calculated for both the observed data and predictions using the first-order transition probability (Haan, 1977) and the numbers of events per year with specific wet/dry spell durations were estimated over the study area for both the wet and dry seasons to investigate precipitation occurrence patterns.

In terms of spatial features, observations and predictions were evaluated using several indices indicating spatial standard deviation, correlation, and variability (Hubert et al., 1981). The Moran's I (Moran, 1950; Thomas and Huggett, 1980) index, a commonly used statistical index for identifying spatial dependence, was calculated using the following formula.

$$I_t = \frac{N}{\sum_i \sum_j w_{ij}} \frac{\sum_i \sum_j w_{ij} \left(x_{t,i} - \overline{x_t}\right)\left(x_{t,j} - \overline{x_t}\right)}{\sum_i \left(x_{t,i} - \overline{x_t}\right)^2} \tag{8}$$

where $x_{t,i}$ and $x_{t,j}$ refer to the precipitation in station i and j on day t, respectively. $\overline{x_t}$ is the overall spatial mean precipitation on day t. w_{ij} is an adjacency weight based on inverse distance weighting. The I values are between -1 and 1. Like the correlation coefficient, I is positive if both $x_{t,i}$ and $x_{t,j}$ lie on the same side of the mean (above or

HESSD
10, 2141–2181, 2013

below), while it is negative if one is above the mean and the other is below the mean (O'Sullivan and Unwin, 2003).

Geary's C (Griffith, 2003) was calculated as a measure of spatial covariance of precipitation among grid cells, as follows:

$$C_t = \frac{(N-1)}{2\sum_i \sum_j w_{ij}} \frac{\sum_i \sum_j w_{ij} \left(x_{t,i} - x_{t,j}\right)^2}{\sum_i \left(x_{t,i} - \overline{x_t}\right)^2} \tag{9}$$

C values range between 0 and 2. The spatial autocorrelation is positive if C is lower than 1, negative if C is between 1 and 2, and zero if C is equal to 1.

In this research average I and C indices were calculated for the wet and dry season over the study period from 1961 to 1999. Moran's I_t and Geary's C_t represent measures of spatial autocorrelation for each spatial field at day t, however the relationship between the geographical distance and correlation are not measured by these statistics. We used the variogram, defined as the expected value of the squared difference of the values of the random field separated by distance vector $\boldsymbol{h}$, to describe the degree of spatial variability exhibited by each spatial random field. The experimental variogram $2\gamma(h)$ for the observed and simulated precipitation data was calculated using the following formula (Goovaerts, 1997).

$$2\gamma(h) = \frac{1}{N(h)} \sum_{\alpha=1}^{N(h)} \left[x(u_\alpha) - x(u_\alpha + h)\right]^2 \tag{10}$$

where $N(h)$ denotes the number of pairs of observations separated by distance h, and $x(u_\alpha)$ and $x(u_\alpha + h)$ are the observed or simulated precipitation at locations u_α and $u_\alpha + h$, respectively.

HESSD
10, 2141–2181, 2013

5 Results and discussion

5.1 Evaluation of temporal variability

Gridded annual total precipitation observations, spatially averaged over the state of Florida, ranged from 1048 mm to 1657 mm with a mean of 1343 mm over the study period from 1961 to 1999. The standard deviation of the spatially averaged annual total observation time series was 152 mm. Figure 2 shows the spatially averaged annual total precipitation time series and mean monthly precipitation of gridded observation (Gobs) over the study period. Table 2 compares the mean and standard deviation of observed and predicted spatially averaged annual precipitation. The BCCA method underestimated the observed mean annual precipitation over the study period by 8 % (CGCM3) to 11 % (CNRM-CM3) while the rest of methods reproduced the mean annual precipitation, with errors less than ±20 mm (< 2 % of observed mean annual precipitation). The temporal standard deviation was slightly underestimated by the BCSD results (114 mm to 147 mm over the GCMs) and BCCA (128 mm to 147 mm), and overestimated by SDBC results (153 mm to 247 mm). The SDBC method overestimates the temporal standard deviation of spatially averaged annual total precipitation because the large-scale daily GCM precipitation predictions are spatially disaggregated by interpolation and then bias-correction at the downscaled grid resolution. Thus each fine-scale grid cell preserves the precipitation percentile event predicted by the large-scale GCM, exaggerating the spatial extent of high and low percentile events. Note that predicted annual time series from GCMs are not expected to reproduce the actual annual time series for the study period since they do not use actual observed initial conditions or boundary conditions in the simulations.

Figures 3 and 4 compare the spatial distribution of mean precipitation for the wet (June to September) and dry seasons (October through May) over the study period and show that mean climatology was accurately reproduced over the state of Florida by the BCSD_daily, SDBC, and BCSA methods. These results are expected since the CDF mapping bias-correction technique employed in these methods is designed to fit

HESSD
10, 2141–2181, 2013

the predictions to historic mean climatology. Meanwhile, the BCCA results accurately reproduced the spatial pattern of observed mean precipitation for both seasons, but slightly overestimated mean precipitation in the southern part of the state in the wet season and underestimated over the entire state in the dry season.

The spatial distribution of the temporal standard deviation of precipitation however, showed significant differences among the downscaling methods. Figures 5 and 6 compare the spatial distribution of the temporal standard deviation of the daily precipitation time series over the state of Florida for the wet and dry seasons over the study period, respectively. While the SDBC and BCSA results accurately reproduced the standard deviation for both the wet and dry seasons, the BCSD_daily results significantly underestimated the standard deviation for both seasons. The BCCA results improved over the BCSD_daily results but still under-predicted the daily precipitation standard deviation because the linear regression scheme used to construct the analogs in BCCA attenuates extreme events and thus decreases temporal variance.

Figures 7 and 8 show the spatial distributions of 90th percentile (5 mm ~ 20 mm) and 50th percentile (< 3 mm) daily precipitation for the wet season, respectively. The results show that the BCSD_daily and BCCA method underestimated the observed 90th percentile daily precipitation amount and overestimated the 50th percentile of daily precipitation because of their tendency to overestimate the occurrence of small rainfall events. Note that BCCA exhibits better skill than BCSD_daily in reproducing 50th percentile of daily precipitation amount but still overestimates compared to observations. On the other hand the SDBC and BCSA method accurately reproduce both the 90th percentile and 50th percentile daily precipitation.

The inaccuracies in the temporal variability produced by the BCSD_daily method are caused by the interpolation scheme that is used to disaggregate the bias corrected GCM predictions which produces smooth downscaled results. Note that the temporal standard deviation at downscaled locations corresponding to the center point of the GCM grid produces slightly higher temporal variability (Figs. 5 and 6) because the interpolation procedure produces less smoothing at these locations. This weakness of the BCSD_daily method is improved by exchanging the order of the bias-correction and interpolation procedures (i.e. SDBC) as shown in Figs. 5 through 8. When the interpolated GCM results are bias-corrected using fine scale gridded observations at the last step of the downscaling process, the final results reproduce the full observed CDF and thus both the observed temporal mean and temporal standard deviation. Although SDBC has been recently introduced for downscaling daily GCM products (Abatzoglou and Brown, 2012), explicit insight into these distinctions between the BCSD_daily and SDBC downscaling frameworks was not provided by the previous studies.

In addition to reproducing temporal statistics of daily rainfall, day to day precipitation patterns are also important for most hydrologic applications. The differences in precipitation occurrence between local and coarse grid scale precipitation series are quite large because precipitation at the coarse grid scale is non-zero when precipitation occurs at any location within the grid cell. Due to this spatial averaging process, the probability of precipitation occurrence for area-averaged time series is necessarily larger than the corresponding probabilities at any point within the coarse grid cell. Daily transitions between wet and dry states estimated for the observed gridded data and the downscaled GCM predictions obtained using the BCSD_daily, BCCA, SDBC, and BCSA methods are shown in Figs. 9 and 10. The BCSD_daily results produced more low rainfall events and thus wet to wet transition probabilities (P_{11}) were overestimated and dry to wet probabilities (P_{01}) were underestimated for this method. P_{11} and P_{01} for the BCCA results are closer to the observed transition probabilities than the BCSD_daily results but are not as accurate as the SDBC and BCSA results. It should be noted that the difference of transition probabilities among the GCMs were not significant for any of the downscaling methods.

The frequency and duration of consecutive wet and dry days reflect dynamic properties of precipitation that have important implications for producing extreme hydrologic behavior (i.e. flood and drought events). For evaluation purposes a wet spell was defined as the length of a period of consecutive wet days ($P > 0.1$ mm) that were preceded and followed by a dry day, and a dry spell was defined as the length of a period of consecutive dry days ($P \leq 0.1$ mm) that were preceded and followed by a wet day. The average number of specific wet and dry spell events over the study period for gridded observation and predictions are compared in Fig. 11. The results indicate that BCSD_daily and BCCA results have fewer events for 5 to 15 wet and dry spell lengths during the wet season. This is because both methods produced too many wet days (> 0.1 mm) and thus fewer total number of events. In contrast, the SDBC and BCSA methods reproduced wet and dry spell lengths much more accurately for all GCMs. Note that the difference in the results obtained by different downscaling techniques is larger than the difference obtained from different GCMs using the same downscaling technique.

5.2 Evaluation of spatial variability

Figure 12 compares the relationship between the spatial standard deviation and mean of daily precipitation events for Gobs and predictions downscaled using the four methods. The results indicate that the observed relationship between spatial variability and event size was reproduced fairly well by the all methods, but that the BCSA method reproduced the relationship more accurately than the other methods. The spatial variability of daily Gobs and downscaled GCMs were quantified also by calculating the average Moran's I and Geary's C for each month (Fig. 13). In general the BCSD_daily and SDBC results produced precipitation fields with overestimated spatial correlation (high Moran I, i.e. ~ 0.4 and 0.3, respectively, compared to ~ 0.2 for observations) and underestimated spatial variance (low Geary's C, i.e. $\sim 0.4 \sim 0.5$ compared to $0.6 \sim 0.8$ for observations). The BCCA results showed better skills than the BCSD_daily and SDBC results for both the Moran's I and Geary's C indices, but was not as accurate as the BCSA method. Note that the spatial variance of precipitation (Geary's C index) was found to show strong seasonality, i.e. higher in the wet season and lower in the dry season. No significant seasonality in spatial correlation (Moran's I) was found.

Figure 14 compares wet season and dry season variograms calculated for each downscaled result to the variograms of the gridded observations. These figures indicate

HESSD
10, 2141–2181, 2013

A stochastic analog downscaling method

S. Hwang and W. D. Graham

that the BCSD method significantly underestimated the observed variogram at all separation distances for both wet (June through September) and dry (October through May) seasons. The BCCA and SDBC variogram improved over the BCSD results, but still underestimated the observed variogram. As designed, the BCSA results reproduced the pattern and magnitude of observed variograms accurately for both seasons.

5.3 Discussion

Overall, the existing interpolation-based statistical downscaling methods (i.e. BCSD_daily, SDBC) and historical analog method (i.e. BCCA) showed limited skills in reproducing temporal and spatial variability of daily precipitation. The skill of the BCSA method improved over these methods. The BCSA method can be applied to downscale coarse resolution climate data into any temporal (e.g. monthly, sub-daily) and spatial scale (e.g. gridded or irregularly distributed points) wherever observations are available to estimate the cumulative distribution functions and spatial correlation structure of precipitation. Additionally, because it generates an ensemble of possible local-scale precipitation patterns the uncertainty due to the downscaling process could be examined using a collection of equally probably downscaled climate fields. The procedure can also be applied to temperature and other surface-weather variables.

One drawback of using the BCSA technique is that spatial disaggregation of coarse scale precipitation prediction is conducted independently on a daily basis, not taking into account day to day, week to week or seasonal temporal relationships at the local scale. Thus the temporal trends and persistence of downscaled precipitation results depend on the large scale bias-corrected GCMs' skill to reproduce the temporal correlation of precipitation patterns. Nonetheless we found that the observed transition probabilities and wet and dry spell lengths were reasonably reproduced by the BCSA method. These results indicate that the GCMs have acceptable skill in representing plausible temporal precipitation patterns.

HESSD
10, 2141–2181, 2013

S. Hwang and W. D. Graham

6 Summary and conclusions

This study developed a new technique (i.e. bias-correction and stochastic analog method, BCSA) to downscale bias-corrected daily GCM precipitation predictions to accurately reproduce observed temporal and spatial statistics. Four GCM results were used to examine the skill of the new downscaling technique for reproducing local temporal mean, standard deviation, 90th ($5 \sim 20$ mm) and 50th (< 3 mm) percentile daily precipitation, wet to wet and wet to dry transition probabilities and the length of wet and dry spell compared to the gridded observations, compared to the BCSD_daily, BCCA, and SDBC downscaling techniques. Downscaled GCM results using BCSD_daily, SDBC, and BCSA accurately reproduced the temporal mean of the daily precipitation as well as the annual cycle of monthly mean precipitation while the BCCA results showed underestimation of the mean daily precipitation. The temporal standard deviation and the magnitude of 90th percentile daily precipitation were underestimated by the BCSD_daily method especially for the wet season. Furthermore the BCSD_daily overestimated low precipitation frequency and wet to wet transition probabilities and underestimated dry to wet transition probabilities. These inaccuracies of the BCSD_daily results in reproducing temporal variability of daily precipitation at the fine-grid scale were improved by the BCCA and SDBC method. However the BCCA method underestimated and the SDBC method overestimated the temporal standard deviation of spatially averaged precipitation. The BCSA reproduced the observed temporal standard deviation, magnitudes of both high (90th percentile) and low (50th percentile) rainfall amounts and wet to wet transition probabilities more accurately than the BCSD_daily and the BCCA method.

More significantly, the interpolation-based downscaling methods (both BCSD_daily and SDBC) were unable to reproduce the observed spatial variability of daily precipitation, which may have important implications for predicting hydrologic behavior in low-relief rain-dominated watersheds (Hwang et al., 2011). The BCCA method was also unable to accurately reproduce the spatial variability of daily precipitation. The

HESSD
10, 2141–2181, 2013

BCSA technique was designed to generate daily precipitation fields that accurately reproduce observed spatial correlation of daily rainfall. Analysis of spatial standard deviation, Moran's I, Geary's C, and variograms quantitatively showed that BCSA is superior in reproducing the spatial variance and correlation of observed daily precipitation compared to the other methods.

This study underscores the need to carefully select a downscaling method that reproduces all precipitation characteristics important for the hydrologic system under consideration if local hydrologic impacts of climate variability and change are going to be accurately predicted. For low-relief, rainfall-dominated watersheds where reproducing small-scale spatiotemporal precipitation variability is important, it is anticipated that the BCSA method will produce superior results over the BCSD, BBCA, or SDBC methods. The next phase of this work will examine the relative abilities of these statistical methods to reproduce historic hydrologic behavior in low-relief rain-dominated watersheds in Florida using an integrated hydrologic model using retrospective GCM simulations. Ultimately the most promising technique will be used to downscale both retrospective GCM predictions and future GCM climate projections, and to use these results with an integrated hydrologic model, to assess potential climate change impacts on regional hydrology.

Acknowledgements. We acknowledge the modeling groups, the Program for Climate Model Diagnosis and Intercomparison (PCMDI) and the WCRP's Working Group on Coupled Modelling (WGCM) for their roles in making available the WCRP CMIP3 multi-model dataset. Support of this dataset is provided by the Office of Science, US Department of Energy. We also acknowledge "bias corrected and downscaled WCRP CMIP3 climate projections" for providing the BCCA results.

HESSD

10, 2141–2181, 2013

References

Abatzoglou, T. J. and Brown, J. T.: A comparison of statistical downscaling methods suited for wildfire applications, Int. J. Climatol., 32, 772–780, doi:10.1002/joc.2312, 2012.

Allen, M. R. and Ingram, W. J.: Constraints on future changes in climate and the hydrologic cycle, Nature, 419, 224–232, 2002.

Andréasson, J., Bergström, S., Carlsson, B., Graham, L. P., and Lindström, G.: Hydrological change-climate change impact simulations for Sweden, J. Human Environ., 33, 228–234, 2004.

Christensen, J. H. and Christensen, O. B.: Severe summertime flooding in Europe, Nature, 421, 805–806, 2003.

Christensen, N. S., Wood, A. W., Voisin, N., Lettenmaier, D. P., and Palmer, R. N.: The effects of climate change on the hydrology and water resources of the Colorado River basin, Climatic Change, 62, 33–363, 2004.

Collins, W. D., Bitz, C. M., Blackmon, M. L., Bonan, G. B., Bretherton, C. S., Carton, J. A., Chang, P., Doney, S. C., Hack, J. J., Henderson, T. B., Kiehl, J. T., Large, W. G., McKenna, D. S., Santer, B. D., and Smith, R. D.: The Community Climate System Model Version 3 (CCSM3), J. Climate, 19, 2122–2143, 2006.

Delworth, T. L., Broccoli, A. J., Rosati, A., et al.: GFDL's CM2 global coupled climate models part 1: formulation and simulation characteristics, J. Climate, 19, 643–674, doi:10.1175/JCLI3629.1, 2006.

Deutsch, C. V. and Journel, A. G.: GSLIB, Geostatistical Software Library and User's Guide, 2nd edn., Oxford Univ. Press, New York, 139–148, 1998.

Dibike, B. Y. and Coulibaly, P.: Hydrologic impact of climate change in the Saguenay watershed: comparison of downscaling methods and hydrologic models, J. Hydrol., 307, 145–163, doi:10.1016/j.jhydrol.2004.10.012, 2005.

Feddersen, H. and Andersen, U.: A method for statistical downscaling of seasonal ensemble predictions, Tellus A, 57, 398–408, 2005.

Flato, G. M. and Boer, G. J.: Warming asymmetry in climate change simulations, Geophys. Res. Lett., 28, 195–198, 2001.

Fowler, H. J., Blenkinsop, S., and Tebaldi, C.: Linking climate change modeling to impacts studies: recent advances in downscaling techniques for hydrological modeling, Int. J. Climatol., 27, 1547–1578, 2007.

HESSD
10, 2141–2181, 2013

A stochastic analog downscaling method

S. Hwang and W. D. Graham

Furevik, T., Bentsen, M., Drange, H., Kindem, I. K. T., Kvamsto, N. G., and Sorteberg, A.: Description and evaluation of the bergen climate model: ARPEGE coupled with MICOM, Clim. Dynam., 21, 27–51, 2003.
Giorgi, F., Hewitson, B., Christensen, J., Hulme, M., Von Storch, H., Whetton, P., Jones, R., Mearns, L., and Fu, C.: Regional climate information-evaluation and projections, in: Climate Change 2001: The Scientific Basis, edited by: Houghton, J. T., Ding, Y., Griggs, D. J., Noguer, M., van der Linden, P. J., Dia, X., Maskell, K., Johnson, C. A., Cambridge University Press, Cambridge, 583–638, 739–768, 2001.
Goovaerts, P.: Geostatistics for Natural Resources Evaluation, Oxford Univ. Press, New York, 3–7, 27–36, 127–139, 152–157, 1997.
Graham, L. P., Hagemann, S., Jaun, S., and Beniston, M.: On interpreting hydrological change from regional climate models, Climatic Change, 81, 97–122, doi:10.1007/s10584-006-9217-0, 2007.
Griffith, D. A.: Spatial Autocorrelation and Spatial Filtering: Gaining Understanding Through Theory and Scientific Visualization, Advances in Spatial Science, Springer, 247 pp., 2003.
Haan, T. C.: Statistical Methods in Hydrology, The Iowa State Univ. Press, Ames, Iowa, 303–305, 1977.
Hay, L. E., Clark, M. P., Wilby, R. L., Gutowski, W. J., Leavesley, G. H., Pan, Z., Arritt, R. W., and Takle, E. S.: Use of regional climate model output for hydrologic simulations, J. Hydrometeorol., 3, 571–590, 2002.
Hidalgo, H. G., Dettinger, M. D., and Cayan, D. R.: Downscaling with constructed analogues: daily precipitation and temperature fields over the United States, California Energy Commission, PIER EnergyRelated Environmental Research, CEC5002007123, 2008.
Hubert, L. J., Golledge, R. G., and Costanzo, C. M.: Generalized procedures for evaluating spatial autocorrelation, Geogr. Anal., 13, 224–233, 1981.
Hwang, S., Graham, D. W., Hernández, L. J., Martinez, C., Jones, W. J., and Adams, A.: Quantitative spatiotemporal evaluation of dynamically downscaled MM5 precipitation predictions over the Tampa Bay region, Florida, J. Hydrometeorol., 12, 1447–1464, 2011.
Ines, A. V. M. and Hansen, J. W.: Bias-correction of daily GCM rainfall for crop simulation studies, Agr. Forest Meteorol., 138, 44–53, 2006.
Intergovernmental Panel on Climate Change (IPCC): Climate Change 2007: The Physical Science Basis, Contribution of Working Group I to the Fourth Assessment Report of the Intergovernmental Panel on Climate Change, edited by: Solomon, S., Qin, D., Manning, M.,

Chen, Z., Marquis, M., Averyt, K. B., Tignor, M., and Miller, H. L., Cambridge Univ. Press, Cambridge, UK, 2007.
Johns, T., Durman, C., Banks, H., Roberts, M., McLaren, A., Ridley, J., Senior, C., Williams, K., Jones, A., Keen, A., Rickard, G., Cusack, S., Joshi, M., Ringer, M., Dong, B., Spencer, H., Hill, R., Gregory, J., Pardaens, A., Lowe, J., Bodas-Salcedo, A., Stark, S., and Searl, Y.: HadGEM1-Model description and analysis of preliminary experiments for the IPCC Fourth Assessment Report, Tech. Note 55, Hadley Center, Exeter, UK, 2004.
K-1 model developers: K-1 coupled model (MIROC) description, K-1 technical report, 1., edited by: Hasumi, H. and Emori, S., Center for Climate System Research, University of Tokyo, 34 pp., 2004.
Karl, R. T. and Trenberth, E. K.: Modern global climate change, Science, 302, 1719–1723, doi:10.1126/science.1090228, 2003.
Katz, R. W. and Zheng, X.: Mixture model for overdispersion of precipitation, J. Climate, 12, 2528–2537, doi:10.1175/1520-0442(1999)012<2528:MMFOOP>2.0.CO;2, 1999.
Lettenmaier, D. P., Wood, A. W., Palmer, R. N., Wood, E. F., and Stakhiv, E. Z.: Water resources implications of global warming: a U.S. regional perspective, Climatic Change, 43, 537–579, 1999.
Maurer, E. P.: Uncertainty in hydrologic impacts of climate change in the Sierra Nevada, California, under two emissions scenarios, Climatic Change, 82, 309–325, doi:10.1007/s10584-006-9180-9, 2007.
Maurer, E. P. and Hidalgo, H. G.: Utility of daily vs. monthly large-scale climate data: an intercomparison of two statistical downscaling methods, Hydrol. Earth Syst. Sci., 12, 551–563, doi:10.5194/hess-12-551-2008, 2008.
Maurer, E. P., Wood, A. W., Adam, J. C., Lettenmaier, D. P., and Nijssen, B.: A long-term hydrologically-based data set of land surface fluxes and states for the conterminous United States, J. Climate, 15, 3237–3251, 2002.
Maurer, E. P., Hidalgo, H. G., Das, T., Dettinger, M. D., and Cayan, D. R.: The utility of daily large-scale climate data in the assessment of climate change impacts on daily streamflow in California, Hydrol. Earth Syst. Sci., 14, 1125–1138, doi:10.5194/hess-14-1125-2010, 2010.
Mearns, L. O., Mavromatis, T., Tsvetsinskaya, E., Hays, C., and Easterling, W.: Comparative responses of EPIC and CERES crop models to high and low resolution climate change scenarios, J. Geophys. Res., 104, 6623–6646, 1999.

Mearns, L. O., Easterling, W., Hays, C., and Marx, D.: Comparison of agricultural impacts of climate change calculated from high and low resolution climate model scenarios: Part I. the uncertainty of spatial scale, Climatic Change, 51, 131–172, 2001.
Moran, P. A. P.: Notes on continuous stochastic phenomena, Biometrika, 37, 17–23, 1950.
Murphy, J.: An evaluation of statistical and dynamical techniques for downscaling local climate, J. Climate, 12, 2256–2284, 1999.
O'Sullivan, D. and Unwin, J. D.: Geographic Information Analysis, Wiley & Sons, Inc., Hoboken, New Jersey, 2003.
Panofsky, H. A. and Brier, G. W.: Some applications of statistics to meteorology, The Pennsylvania State University, University Park, PA, USA, 224 pp., 1968.
Salas-Mélia, D., Chauvin, F., Déqué, M., Douville, H., Guérémy, J. F., Marquet, P., Planton, S., Royer, J. F., and Tyteca, S.: Description and validation of the CNRM-CM3 global coupled model, CNRM Working Note 103, 36 pp., 2005.
Salathe, E. P., Mote, P. W., and Wiley, M. W.: Review of scenario selection and downscaling methods for the assessment of climate change impacts on hydrology in the United States pacific northwest, Int. J. Climatol., 27, 1611–1621, doi:10.1002/joc.1540, 2007.
Shepard, D. S.: Computer mapping: the SYMAP interpolation algorithm, in: Spatial Statistics and Models, edited by Gaile, G. L., Willmott, C. J., and Reidel, D., Norwell, Mass., 133–145, 1984.
Smith, M., Koren, V., Zhang, Z., Reed, S., Pan, J.-J., and Moreda, F.: Runoff response to spatial variability in precipitation: an analysis of observed data, J. Hydrol., 298, 267–286, 2004.
Taussky, O. and Todd, J.: Cholesky, Toeplitz and the triangular factorization of symmetric matrices, Numer. Algorithms, 41, 197–202, 2006.
Thomas, R. W. and Huggett, R. J.: Modelling in Geography: a Mathematical Approach, Barns & Noble Books, New Jersey, 1980.
Timbal, B., Fernandez, E., and Li, Z.: Generalization of a statistical downscaling model to provide local climate change projections for Australia, Environ. Model. Softw., 24, 341–358, 2009.
Wilby, R. L. and Wigley, T. M. L.: Downscaling general circulation model output: a review of methods and limitations, Prog. Phys. Geogr., 21, 530–548, 1997.
Wilby, R. L., Charles, S. P., Zorita, E., Timbal, B., Whetton, P., and Mearns, L. O.: Guidelines for use of climate scenarios developed from statistical downscaling methods, Tech. rep., IPCC, 2004.

Wilks, D. S.: Multisite downscaling of daily precipitation with a stochastic weather generator, Clim. Res., 11, 125–136, 1999.
Wilks, D. S.: Realizations of daily weather in forecast seasonal climate, J. Hydrometeorol., 3, 195–207, doi:10.1175/1525-7541(2002)003<0195:RODWIF>2.0.CO;2, 2002.
Wood, A. W., Maurer, E. P., Kumar, A., and Lettenmaier, D. P.: Long-range experimental hydrologic forecasting for the eastern United States, J. Geophys. Res., 107, 4429, doi:10.1029/2001JD000659, 2002.
Wood, A. W., Leung, L. R., Sridhar, V., and Lettenmaier, D. P.: Hydrologic implications of dynamical and statistical approaches to downscaling climate model outputs, Climatic Change, 15, 189–216, 2004.
Yang, T., Li, H., Wang, W., Xu, C.-Y., and Yu, Z.: Statistical downscaling of extreme daily precipitation, evaporation, and temperature and construction of future scenarios, Hydrol. Process., 26, 3510–3523, doi:10.1002/hyp.8427, 2012.
Zhang, F. and Geogakakos, P. A.: Joint variable spatial downscaling, Climatic Change, 111, 945–972, 2012.
Zorita, E. and von Storch, H.: The analog method as a simple statistical downscaling technique: comparison with more complicated methods, J. Climate, 12, 2474–2489, 1999.

HESSD
10, 2141–2181, 2013

Title Page
Abstract | Introduction
Conclusions | References
Tables | Figures
◀| |▶
◀ ▶
Back | Close
Full Screen / Esc
Printer-friendly Version
Interactive Discussion

Table 1. GCMs considered in this study.

Modeling Group, Country	WCRP CMIP3[a] I.D.	Primary Reference
Bjerknes Centre for Climate Research, Norway	**BCCR-BCM2.0**	Furevik et al. (2003)
US Dept. of Commerce/NOAA/Geophysical Fluid Dynamics Laboratory, USA	**GFDL-CM2.0**[b]	Delworth et al. (2006)
Canadian Centre for Climate Modeling & Analysis, Canada	**CGCM3.1**[b]	Flato and Boer (2001)
National Center for Atmospheric Research, USA	**CCSM3**	Collins et al. (2006)
Meteo-France/Centre National de Recherches Meteorologiques, France	CNRM-CM3[b]	Salas-Melia et al. (2005)
Center for Climate System Research (The University of Tokyo), National Institute for Environmental Studies, and Frontier Research Center for Global Change, Japan	MIROC3.2[b]	K-1 model developers (2004)

[a] World Climate Research Programme's Coupled Model Inter-comparison Project phase 3.
The GCMs presented bold in the table indicate the models downscaled in this study.
[b] Indicate the models additionally selected for BCCA results for the purpose of comparative evaluation.

HESSD
10, 2141–2181, 2013

HESSD
10, 2141–2181, 2013

A stochastic analog downscaling method

S. Hwang and W. D. Graham

Table 2. The mean and standard deviation of spatially averaged annual total precipitation over the state of Florida for the downscaled GCM results using 4 different statistical downscaling methods.

	The spatially averaged mean annual total precipitation Gobs: 1343 mm				The standard deviation of the spatially averaged annual total precipitation Gobs: 152 mm			
Units: mm Period: 1961 ~ 1999	BCSD_daily	BCCA	SDBC	BCSA	BCSD_daily	BCCA	SDBC	BCSA
BCCR-BCM2.0	1359	–	1356	1356	147	–	233	178
GFDL-CM2.0	1359	1227	1357	1357	165	147	247	187
CGCM3.1	1362	1239	1361	1360	132	128	223	167
CCSM3	1363	–	1361	1359	114	–	153	125
CNRM-CM3	–	1190	–	–	–	133	–	–
MIROC3.2	–	1236	–	–	–	134	–	–

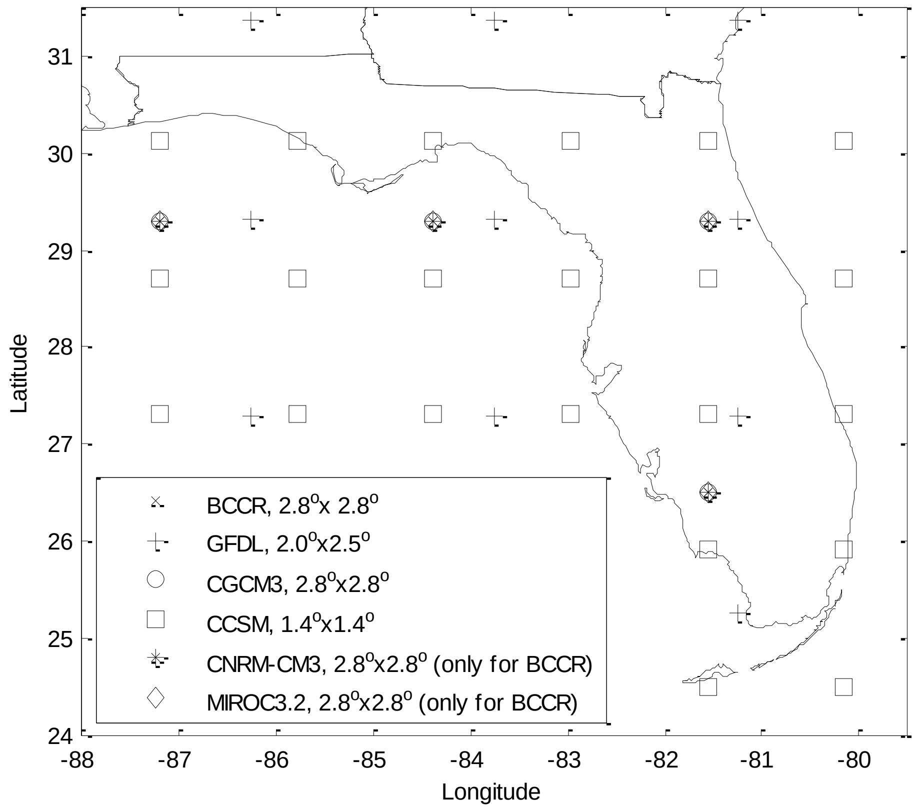

Fig. 1. The study domain and the center location of grids for the GCMs used in the study. Note that the grid resolutions and configurations for BCCR, CGCM3, CNRM-CM3, and MIROC3.2 are identical.

HESSD
10, 2141–2181, 2013

A stochastic analog downscaling method

S. Hwang and W. D. Graham

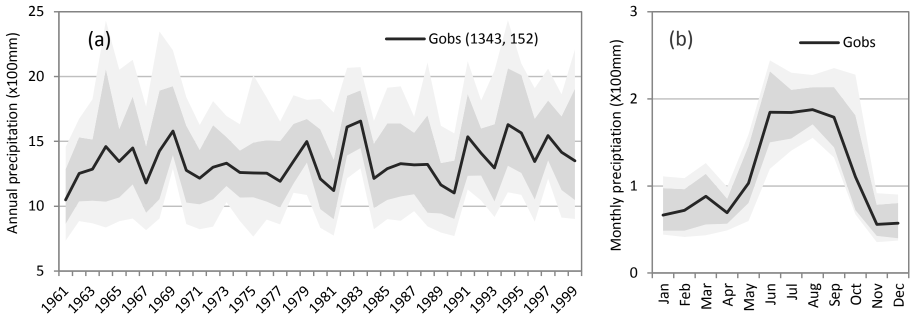

Fig. 2. Comparison of **(a)** spatially averaged annual total precipitation time series and **(b)** the mean monthly precipitation over the study period for gridded observations (Gobs). The bright and dark gray zones represent total data range and 5th to 95th percentile of Gobs at the 12 km grid scale indicating the spatial variability of observed annual total precipitation and the mean monthly precipitation over Florida. Mean and standard deviation of annual preciptiation predictions are represented in the panel. Units in mm.

HESSD
10, 2141–2181, 2013

S. Hwang and W. D. Graham

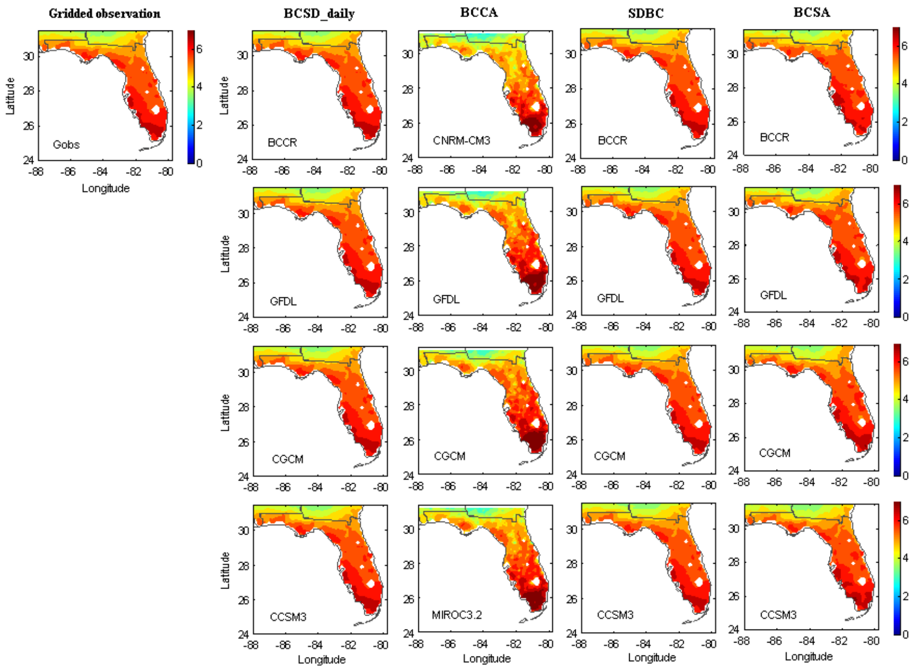

Fig. 3. Spatial distribution of the mean of Gridded observation (Gobs.), BCSD_daily, BCCA, SDBC, and BCSA daily precipitation for wet season (June through September), units in mm.

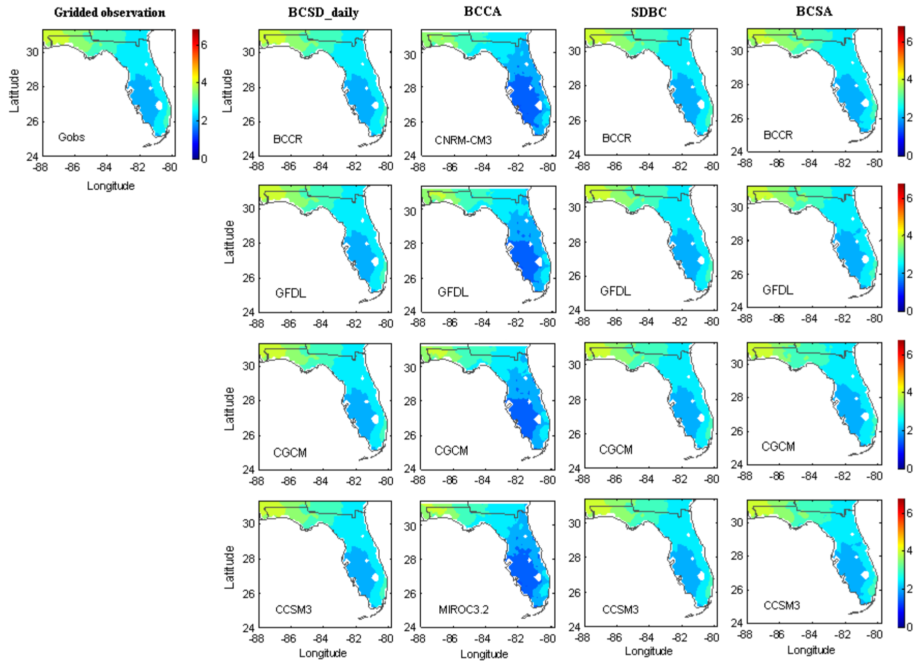

Fig. 4. Spatial distribution of the mean of Gridded observation (Gobs.), BCSD_daily, BCCA, SDBC, and BCSA daily precipitation but for dry season (October through May).

HESSD
10, 2141–2181, 2013

S. Hwang and W. D. Graham

HESSD
10, 2141–2181, 2013

A stochastic analog downscaling method

S. Hwang and W. D. Graham

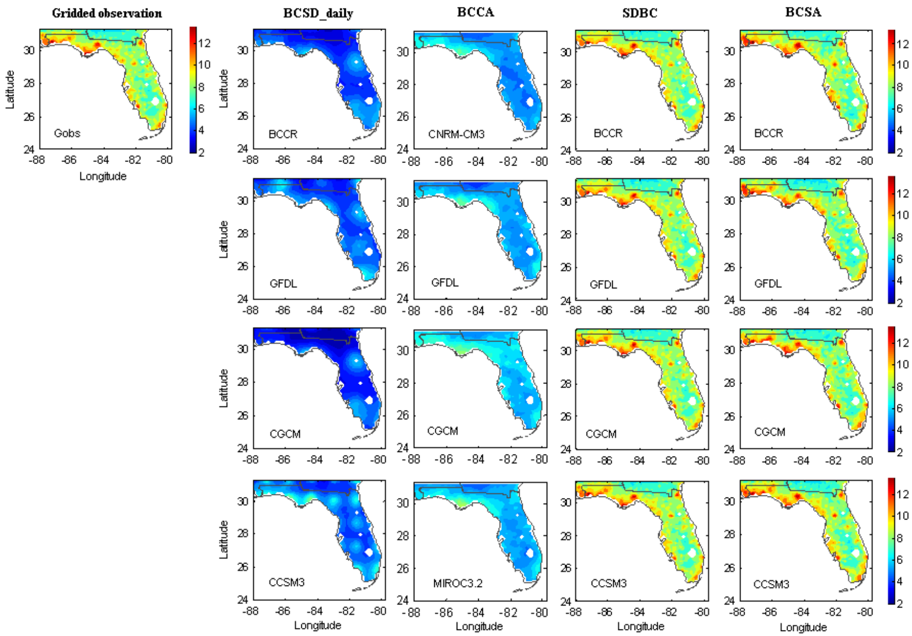

Fig. 5. Spatial distribution of the temporal standard deviation of Gobs., precipitation predictions downscaled using BCSD_daily, BCCA, SDBC, and BCSA for wet season (June through September), units in mm.

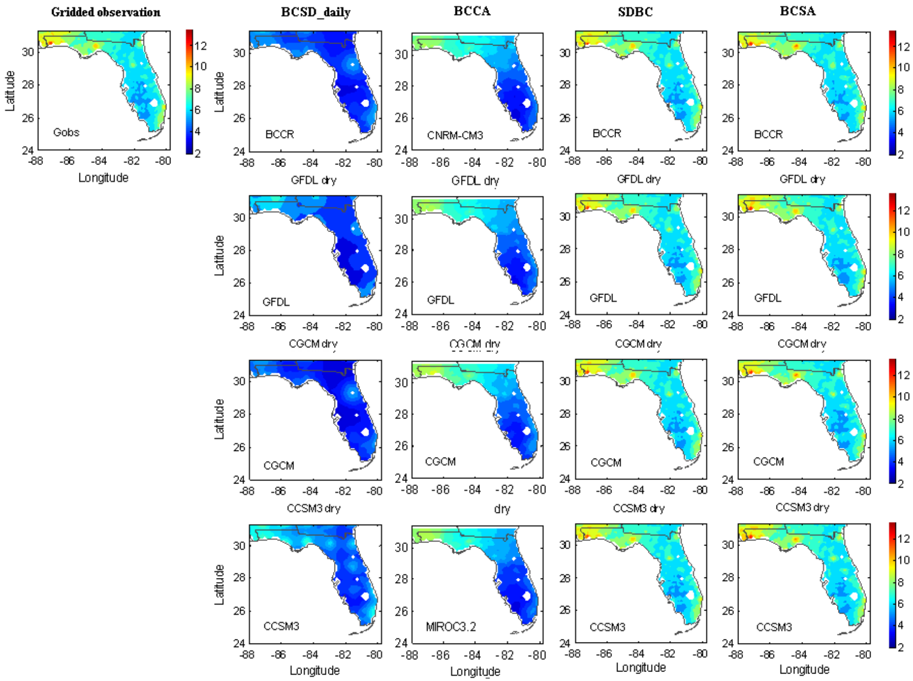

Fig. 6. Spatial distribution of the temporal standard deviation of Gobs., precipitation predictions downscaled using BCSD_daily, BCCA, SDBC, and BCSA for dry season (October through May).

HESSD
10, 2141–2181, 2013

A stochastic analog downscaling method

S. Hwang and W. D. Graham

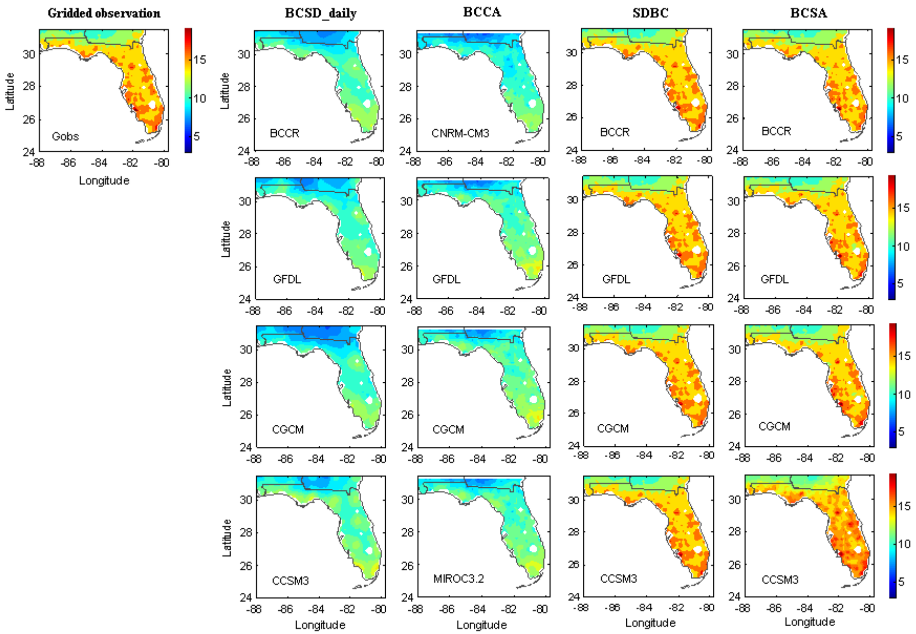

Fig. 7. Spatial distribution of the 90th percentile daily precipitation of Gobs, BCSD_daily, BCCA, SDBC, and BCSA GCMs for each grid cell for wet season (June through September), units in mm.

HESSD
10, 2141–2181, 2013

S. Hwang and W. D. Graham

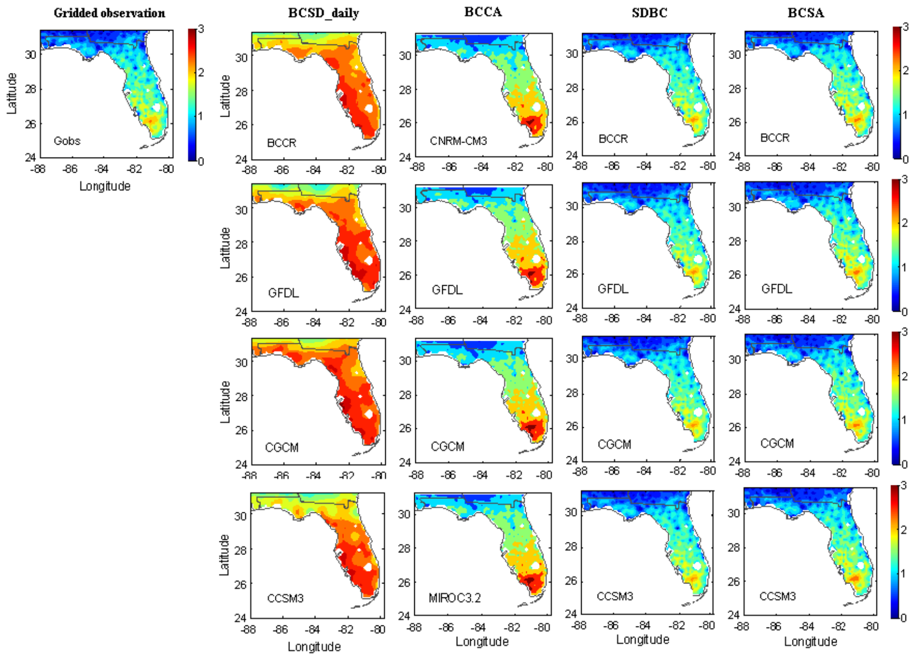

Fig. 8. Spatial distribution of the 50th percentile daily precipitation of Gobs, BCSD_daily, BCCA, SDBC, and BCSA GCMs for each grid cell for wet season (June through September), units in mm.

HESSD
10, 2141–2181, 2013

A stochastic analog downscaling method

S. Hwang and W. D. Graham

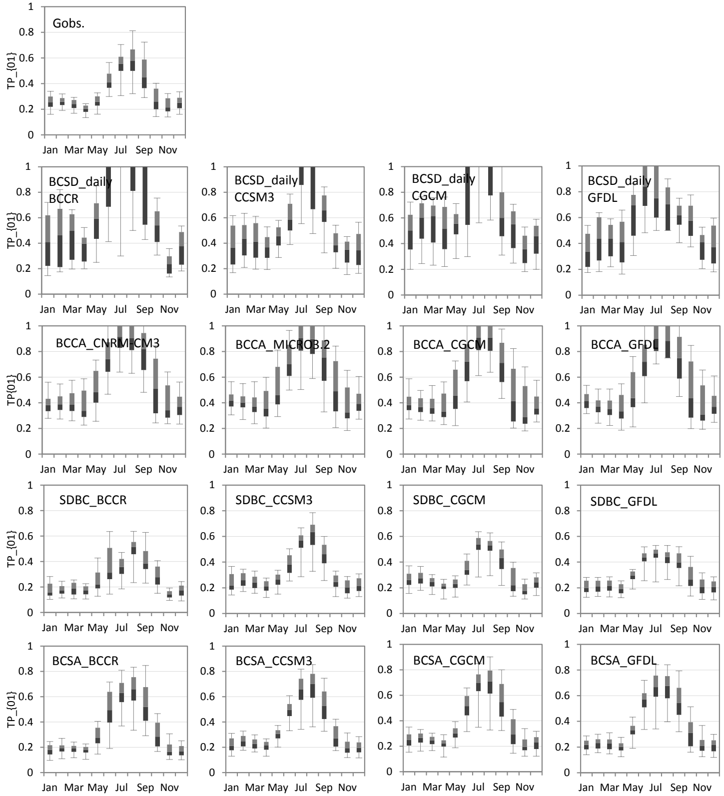

Fig. 9. First-order dry to wet transition probability ($P_{\{01\}}$) comparisons of observation (first row), BCSD_daily results (second row), BCCA results (third row), SDBC (forth row), and BCSA results (fifth row) for each month and 4 GCM products over all grids in the study area. Box plot presents minimum, 10th percentile, median, 90th percentile, and maximum over the grids.

HESSD
10, 2141–2181, 2013

A stochastic analog downscaling method

S. Hwang and W. D. Graham

Title Page
Abstract | Introduction
Conclusions | References
Tables | Figures
◀| |▶
◀ ▶
Back | Close
Full Screen / Esc
Printer-friendly Version
Interactive Discussion

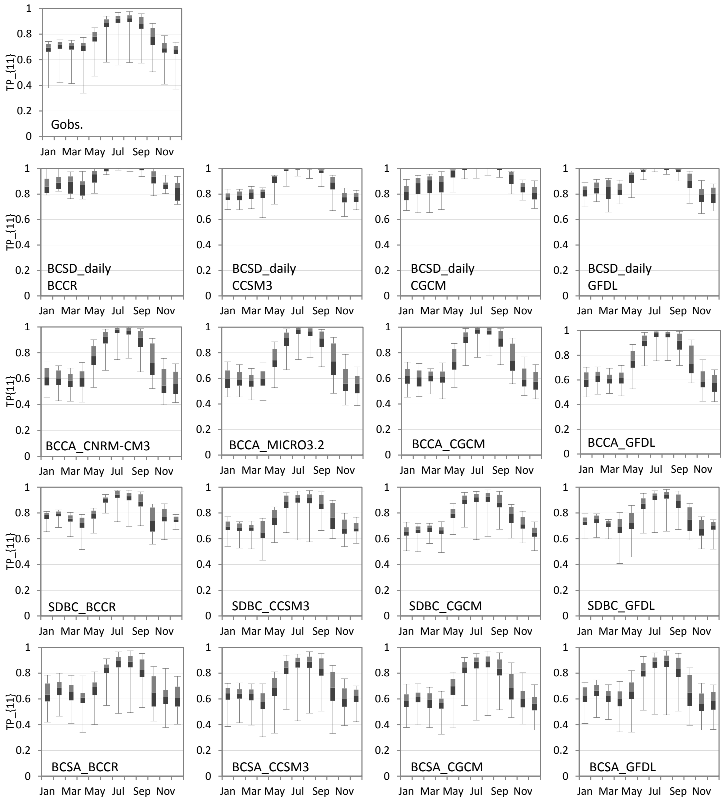

Fig. 10. First-order wet to wet transition probability ($P_{\{11\}}$) comparisons of observation (first row), BCSD_daily results (second row), BCCA results (third row), SDBC (forth row), and BCSA results (fifth row) for each month and 4 GCM products over all grids in the study area. Box plot presents minimum, 10th percentile, median, 90th percentile, and maximum over the grids.

HESSD
10, 2141–2181, 2013

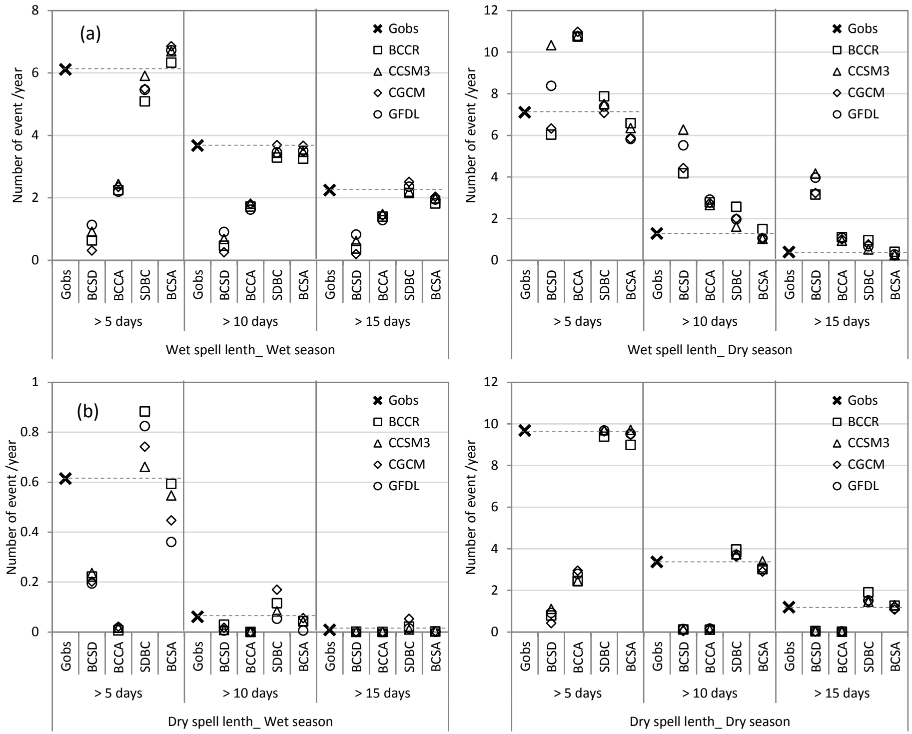

Fig. 11. Number of the events for given **(a)** wet (≥ 0.1 mm) and **(b)** dry (< 0.1 mm) spell lengths (5, 10, and 15 days) for the Gobs. and statistically downscaled GCM results using BCSD_daily, BCCA, SDBC, and BCSA for wet (left column) and dry season (right column). Dotted line indicates the observed exceedence probability. Note that, exceptionally for BCCA results, the markers indicate the GCMs, BCCR and CCSM3 present the CNRM-CM3 and MICRO3.2 results, respectively.

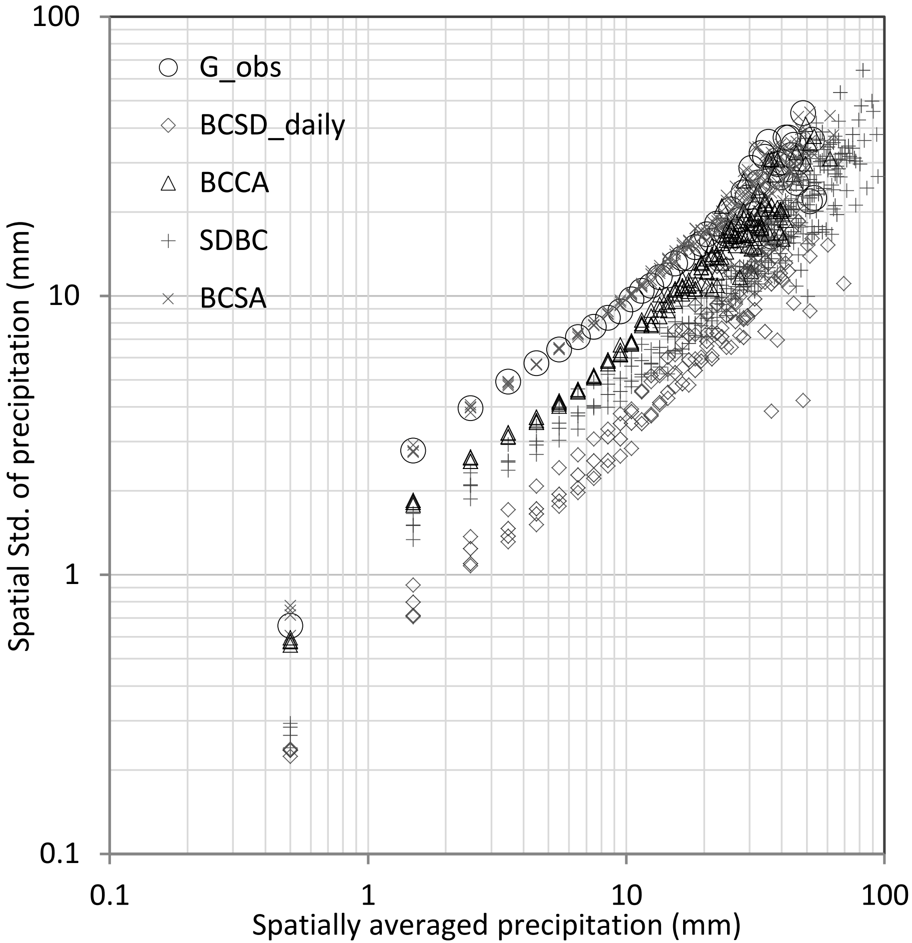

Fig. 12. Comparison of the relationship between spatial standard deviations of daily precipitation and the spatially averaged daily precipitation.

HESSD
10, 2141–2181, 2013

A stochastic analog downscaling method

S. Hwang and W. D. Graham

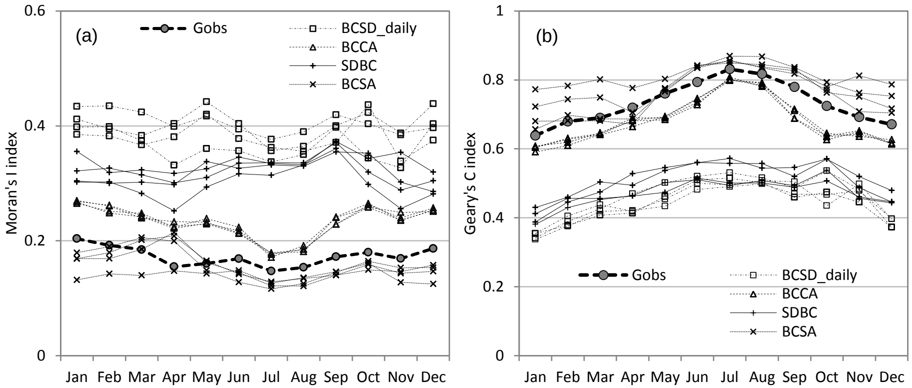

Fig. 13. Comparison of observed and simulated mean daily spatial correlation indices **(a)** / and spatial variance indices **(b)** *C* for each month.

HESSD
10, 2141–2181, 2013

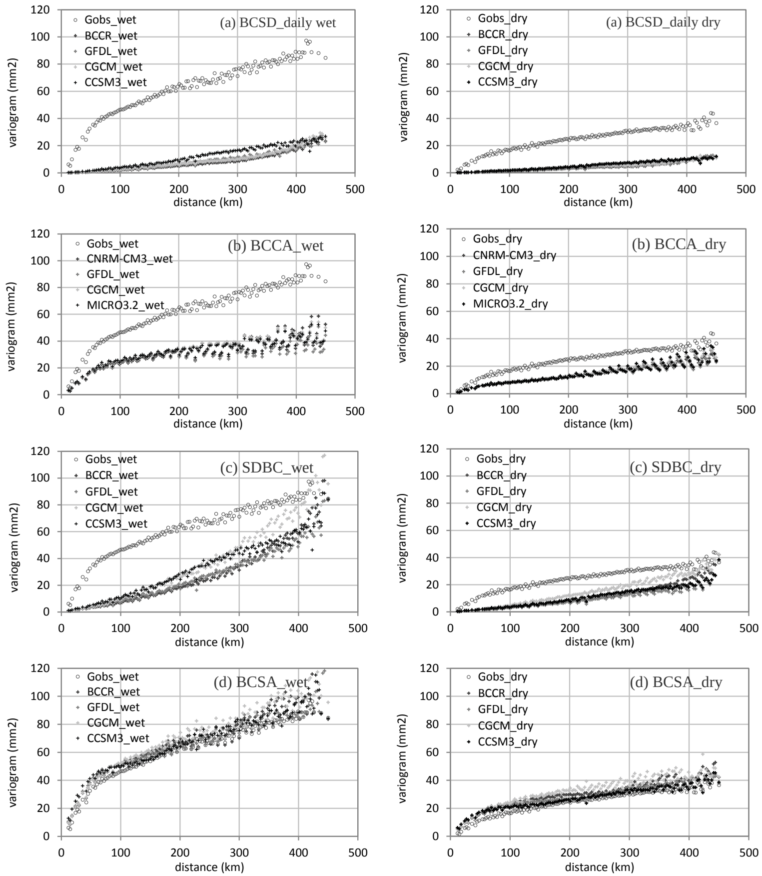

Fig. 14. Variogram comparison of **(a)** BCSD_daily, **(b)** BCCA, **(c)** SDBC, and **(d)** BCSA daily precipitation predictions for wet (left column, June through September) and dry season (right column, October through May).

HESSD
10, 2141–2181, 2013

S. Hwang and W. D. Graham

Title Page
Abstract
Introduction
Conclusions
References
Tables
Figures
◀◀
▶▶
◀
▶
Back
Close
Full Screen / Esc
Printer-friendly Version
Interactive Discussion